Assessing the Influence of Copper Oxide Nanoparticles Combined with Distilled Water on PVT System Performance

M. Ghaderi[1], P. Salami[1*], H. Samimi-Akhijahani[1], S. Zareei[1], M. Safvati[2]

1- Department of Biosystems Engineering, Faculty of Agriculture, University of Kurdistan, Sanandaj, Iran
2- Department of Biosystems Engineering, Faculty of Agriculture, Isfahan University of Technology, Isfahan, Iran
(* Corresponding Author Email: p.salami@uok.ac.ir)
https://doi.org/10.22067/jam.2025.92457.1349

Abstract

The rapid growth of the global population and the increasing demand for energy, coupled with the urgent need for environmental conservation, have prompted researchers to explore renewable energy sources as viable alternatives to non-renewable fossil fuels. This study evaluates the performance enhancement of photovoltaic/thermal (PVT) systems using an immersion cooling method with copper oxide nanofluids. The experimental setup included a glass chamber immersing the panel surface, tested at nanofluid volume ratios of 0.025% and 0.05%, and flow rates of 0.01 and 0.02 L s^{-1}. The immersion height was 5 cm within the glass chamber. The tests were conducted under ambient conditions, which included an ambient temperature of 20.6-31.2 °C and an irradiance of 343-924 W m^{-2}. Results demonstrate that copper oxide nanofluids at a 0.05% volume ratio and a 0.02 L s^{-1} flow rate improved thermal efficiency to 31.87% and reduced panel surface temperature by up to 11.8 °C compared to water cooling. Also, the electrical efficiency of the PVT system exceeded that of the reference panel. The overall efficiency of the PVT system reached 41.89%. These findings highlight the potential of nanofluid-based cooling to optimize PVT system efficiency by enhancing thermal management.

Keywords: Cooling, CuO Nanofluid, Immersion, System temperature, Thermal efficiency

Nomenclature

A_{PV}	Photovoltaic panel area (m^2)	T_r	Reference temperature (°C)
c_p	Specific heat capacity of water (J kg^{-1} $°C^{-1}$)	V_{OC}	Open-circuit voltage (V)
$\dot{E}_{PV}$	Output power of the PV panel (W)		Greek symbols
FF	Fill factor	α_{PV}	Absorptivity coefficient
G	Solar irradiation (W m^{-2})	β_r	Cell temperature coefficient
I_{SC}	Short-circuit current (A)	η_{ele}	Electrical efficiency
$\dot{m}$	Fluid mass flow rate (kg s^{-1})	$\eta_{PV/T}$	Overall efficiency of PVT
$T_{f,in}$	Input fluid temperature (°C)	η_r	Reference (or rated) efficiency of the PV panel under STC
$T_{f,out}$	Output fluid temperature (°C)	η_{th}	Thermal efficiency
T_{PV}	Photovoltaic panel's back surface temperature (°C)	τ_g	Transmittance coefficient

Introduction

The efficiency of power supply systems is critical in the energy sector. In Iran, the emphasis on energy consumption and optimization within energy-intensive systems has traditionally been limited, largely due to the country's abundant fossil fuel resources. However, as these resources become depleted and environmental pollution from their use increases, the Comprehensive National Development Document has established a goal for at least 30% of the country's electricity to be sourced from renewable energy by 2051. Moreover, over half of this renewable energy is expected to come specifically from solar power. Consequently, it is vital to develop and implement systems that can effectively harness renewable energy, either independently or in combination with other energy sources (Mirzaee, Salami, Samimi Akhijahani, & Zareei, 2023, Mohammadi Sarduei,

Mortezapour, & Jafari Naeimi, 2017; Salami, Ajabshirchi, Abdollahpoor, & Behfar, 2016).

Solar power holds tremendous potential for alleviating the impacts of climate change associated with fossil fuel reliance in energy production, making it essential to improve the efficiency of solar energy technologies. Recent findings indicate that photovoltaic systems can compete effectively with fossil fuels. However, a significant challenge is the rise in temperature of solar cells, which adversely affects their electrical performance. To address this issue, researchers have developed an innovative solution to dissipate excess heat from these systems, utilizing nanotechnology to reduce temperatures and enhance electrical efficiency (Ahmed, Baig, Sundaram, & Mallick, 2019; Haidar, Orfi, & Kaneesamkandi, 2018; Sathe & Dhoble, 2017).

A photovoltaic cell is a semiconductor device that generates electric current when exposed to light (Elias, AlSadoon, & Abdulgafar, 2014). Among solar energy technologies, the photovoltaic-thermal system is recognized as the most efficient and widely used today, thanks to its stable, environmentally friendly, secure, and aesthetically pleasing attributes. One effective strategy to improve efficiency and reduce thermal degradation in photovoltaic panels is to lower their surface operating temperature. This can be achieved by implementing cooling methods that minimize heat accumulation in the photovoltaic cells during operation (Brahim & Jemni, 2017; Joshi, Andhare, Bhave, & Gudadhe, 2019; Sheeba, Rao, & Jaisankar, 2015; Siah Chehreh Ghadikolaei, 2021). In their study, Tina, Rosa-Clot, Rosa-Clot, and Scandura (2012) introduced a different photovoltaic cooling solution utilizing a photovoltaic system submerged in shallow water. They discovered that minimizing thermal drift and decreasing reflection contributed to an increase in photovoltaic efficiency of about 15% at a water depth of 4 cm. Idoko, Anaya-Lara, and McDonald (2018) explored the effect of water cooling on the performance of two 250-W solar panels. One panel featured a water-cooling system designed to maintain a surface temperature of 20°C, while the other functioned without any cooling mechanism. Utilizing the PV array power output equation with a derating factor of 80%, they assessed the power output of both panels. The results revealed an increase of 20.96 W in output power and a minimum efficiency improvement of 3% for the water-cooled panel. These findings underscore the substantial advantages of water cooling in enhancing the efficiency and performance of solar panels. Findings from a research study showed that employing a water-cooling technique from the upper surface of the panel enhanced the photovoltaic panel's efficiency by around 0.8-1.5%. The cooling process relies on natural water flow through pipes that contain nozzles placed at regular intervals, channeling water from the top to the bottom of the panel. Furthermore, integrating this system with a flat-plate collector allows for the effective use of the water heated by the panel for domestic purposes (Arefin, 2019).

Nanofluids are innovative fluids that incorporate nanoscale particles suspended in a liquid medium. Their high surface-to-volume ratio provides several benefits, including improved catalytic performance, minimized waste generation in chemical processes, enhanced material strength, and increased thermal conductivity in industrial applications (Amalraj & Michael, 2019; Pordanjani *et al.*, 2021). In photovoltaic (PV) systems, nanofluids are increasingly employed as advanced coolants due to their superior heat transfer properties. For example, circulating nanofluids across PV panels can reduce operating temperatures by 10-20 °C, improving electrical efficiency by 3-15% while simultaneously harvesting thermal energy for secondary applications (Ahmed *et al.*, 2019; Al-Ghezi, Abass, Salam, Jawad, & Kazem, 2021). The photovoltaic-thermal system enhances photovoltaic panel efficiency through nanofluid cooling (Al-Ezzi & Ansari, 2022). In this context, copper oxide (CuO) is a monoclinic semiconducting compound that is

the simplest copper compound and possesses various advantageous physical properties, such as high-temperature superconductivity and spin dynamics. CuO nanofluids are particularly effective in PVT systems due to their high thermal conductivity (~40 W (m K)$^{-1}$) and optical absorption, enabling efficient cooling and waste heat recovery (Alktranee, Shehab, Németh, Bencs, & Hernadi, 2023). It is affordable, combines easily with polar liquids and polymers, and stays stable in chemical and physical contexts (Allaker & Yuan, 2019).

In a study, incorporating 2% nano-CuO into water significantly improved thermal conductivity by 100%. Stability tests indicated high zeta potential across all formulations, with better stability at lower nanoparticle concentrations. Use of nanofluids resulted in greater electrical, thermal, and overall efficiencies compared to traditional cooling methods. The optimal system achieved electrical, thermal, and total efficiencies of 29.92%, 61.08%, and 91%, respectively (Al-Ghezi *et al.*, 2021).

Utilizing TRNSYS simulations, researchers analyzed how CuO nanofluid performs at various concentrations (0.10%-0.50%) and flow rates (60-120 kg h^{-1}) in a PVT system. Results showed that increasing nanofluid concentration and flow rate generally improved electrical and thermal efficiencies, but higher flow rates increased pump power consumption, reducing net efficiency. Optimal performance was achieved at 0.10% concentration and 80 kg h^{-1} flow rate, balancing efficiency gains with minimal power consumption (Madas, Narayanan, & Gudimetla, 2023). In a research, a cooling PVT system with TiO_2-CuO hybrid nanofluid, achieving a 39% reduction in PV cell temperature, was investigated. At 0.3 vol%, electrical power improved by 77.5%, overall efficiency by 58.2%, and exergy efficiency by 14.97%, while exergy losses and entropy generation decreased by 37.9% and 69.6%. The economic analysis revealed a payback period of 21 months compared to systems without cooling (Alktranee *et al.*, 2023). The study improved PVT system performance by using CuO-H_2O nanofluid and a rectangular-cut turbulator. The turbulator enhanced TPV uniformity by 20.43% and increased overall efficiency by 4.99% at high irradiation (G = 930 W m^{-2}). Higher inlet velocity boosted PVT efficiency by 3.19% and TPV uniformity by 16.34%, while increased wind speed decreased PVT efficiency by 3.63% (Khalili & Sheikholeslami, 2024).

This study utilized an innovative technique involving immersing the upper surface of the photovoltaic panel within a glass chamber, allowing the copper oxide nanofluid to enter through the inlets located at the top of the chamber and flow out through the outlets integrated in the lower section of the glass chamber. This approach aimed to enhance the cooling of the photovoltaic panel and boost the overall efficiency of the system. In other words, the study presents a novel approach to enhancing photovoltaic-thermal (PVT) system efficiency through the use of an immersion cooling method with copper oxide nanofluids. Unlike traditional cooling methods using water or air, this innovative technique optimizes thermal management by reducing surface temperatures and increasing thermal efficiency. The research bridges the gap between theoretical studies on nanofluids and practical applications in renewable energy, offering a validated solution to improve PV system performance. By addressing the critical issue of heat dissipation in solar panels, this study provides new insights and actionable strategies for advancing sustainable energy technologies, making it a significant contribution to the field.

Materials and Methods

The photovoltaic-thermal (PVT) system was developed at the Renewable Energy Laboratory at the University of Kurdistan, Iran. Conventional photovoltaic systems employ a variety of silicon materials such as monocrystalline silicon, polycrystalline silicon, and thin-film silicon (amorphous silicon), each demonstrating distinct efficiency ranges. In this study, two monocrystalline

silicon panels were employed: one served as the reference panel while the other was the PVT system. Table 1 shows the specifications of the PV modules.

Table 1- PV module specifications

Specification	Value
Maximum Power (P_{max})	100 W
Voltage at P_{max} (V_{mp})	18.50 V
Current at P_{max} (I_{mp})	5.41 A
Open-Circuit Voltage (V_{oc})	22.20 V
Short-Circuit Current (I_{sc})	5.74 A
Nominal Operating Cell Temperature (NOCT)	47±2 °C
Maximum System Voltage	1000 VDC
Dimensions (mm)	1015 × 668 × 30

The tests were conducted under ambient conditions, which included an ambient temperature of 20.6-31.2 ℃ and an irradiance of 343-924 W m^{-2}. To optimize the system for the panel's specific dimensions and the desired height, a custom glass chamber was constructed to facilitate seamless integration. Additionally, two supporting frames were designed and manufactured, one for the PVT system and the other for the reference panel (as shown in Fig. 1). The experimental setup involved testing at two mass flow rates (0.01 and 0.02 L s^{-1}) for both water and nanofluid, as well as at two concentration levels (0.025% and 0.05%) of the nanofluid, with an immersion height of 5 cm within the glass chamber.

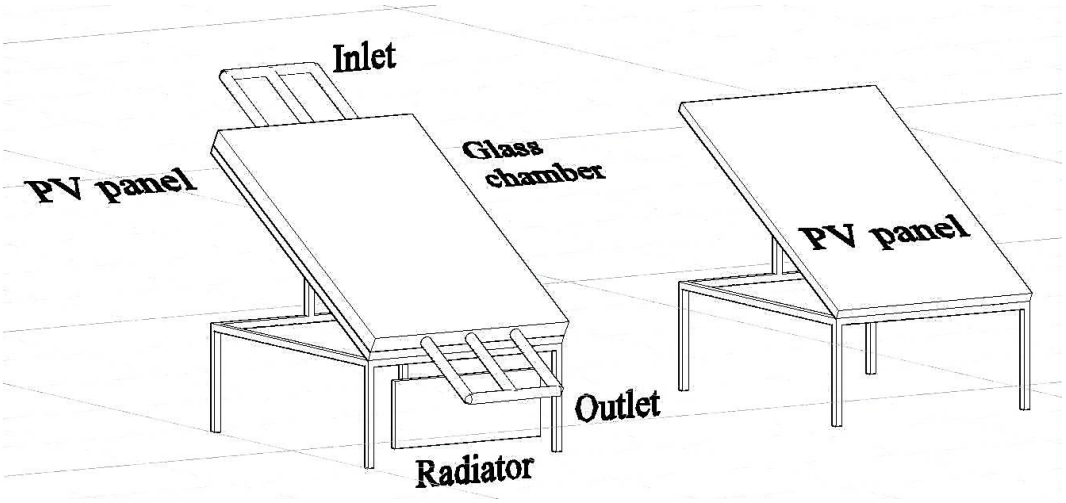

a

b

Fig. 1. The reference panel and PVT system developed in this study: (a) schematic diagram, and (b) the real image

Details of the synthesis of nanofluids and the stability of nanofluids

Enhancing the heat transfer coefficient and thermal efficiency can be achieved by adding nanoparticles, such as Fe, Al, and Cu, to pure water. Based on prior research and the advantages of nanofluids, they are considered a suitable choice for use as working fluids in various types of solar collectors. In this study, a 0.025% and 0.05% nanofluid, consisting of CuO nanoparticles mixed with water, was utilized as the working fluid in the PVT, replacing traditional water.

To prepare the nanofluid, CuO nanoparticles were initially added to water, followed by mixing the solution in a beaker with a hand mixer for one minute. The mixture was then placed in a magnetic stirrer for 20 minutes. Subsequently, the nanofluid underwent ultrasonic homogenization at a frequency of 20 kHz and power of 50 watts for approximately five hours to ensure stability (Fig. 2).

An essential consideration in this process is the prevention of nanofluid deposition within the Photovoltaic Distilled Coolant (PDC) system, as this can reduce thermal efficiency and damage the PVT system. The stability of the nanofluid must therefore be verified. A simple visual observation method was employed by placing the mixture in a container and monitoring it at regular intervals. The results confirmed that the 0.025% and 0.05% water with CuO mixture achieved the desired stability. Over time, no significant differences were observed in the mixture, validating its suitability as a working fluid for the PDC system.

The prevention of nanofluid deposition within the PVT system is crucial, as particle sedimentation can reduce thermal efficiency and potentially damage the system. Thus, in addition to this method, Dynamic Light Scattering (DLS) was used to monitor nanofluid deposition. Particle size distribution and zeta potential measurements were conducted at regular intervals to quantitatively evaluate the colloidal stability of the CuO nanofluid. The zeta potential values remained above -30 mV throughout the testing period, indicating good electrostatic stability.

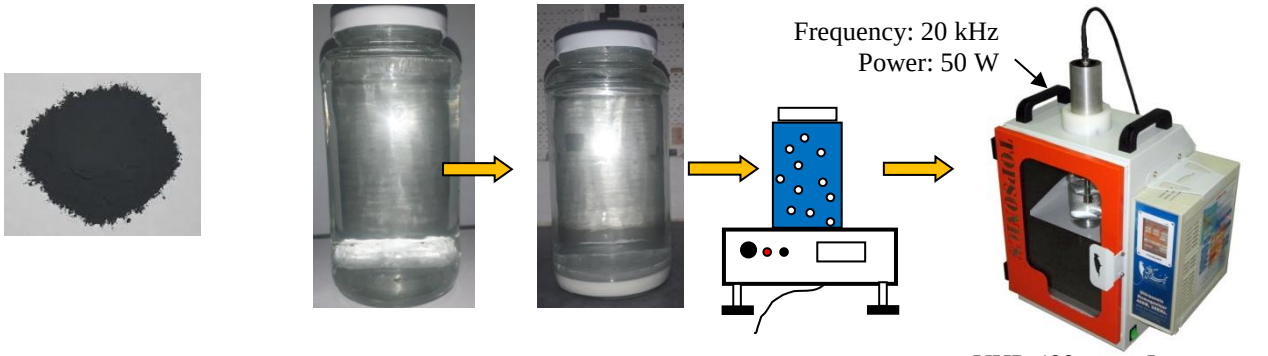

Fig. 2. The steps of preparing the mixture and achieving stability

Ensuring optimal efficiency in solar panels, along with various other factors, is essential for designing an effective photovoltaic system. The performance of a PVT system that utilizes nanofluids can be evaluated using Equations 1 to 3, which take into account thermal, electrical, and overall energy efficiencies (Dubey, Sarvaiya, & Seshadri, 2013; Sardarabadi, Passandideh-Fard, & Zeinali Heris, 2014; Yazdanifard, Ameri, & Ebrahimnia-Bajestan, 2017):

$$\eta_{th} = \frac{\dot{m}c_p(T_{f,out}-T_{f,in})}{G\times A_{PV}} \quad (1)$$

Where, η_{th} = Thermal efficiency (dimensionless); $\dot{m}$ = Mass flow rate (kg s^{-1}); c_p = Specific heat capacity of fluid (J (kg K)$^{-1}$); T_{out} = Outlet fluid temperature (K); T_{in} = Inlet fluid temperature (K); G = Solar irradiance (W m^{-2}); A_{PV} = PV panel area (m^2).

$$\eta_{ele} = \frac{V_{OC}\times I_{SC}\times FF}{G\times A_{PV}} \quad (2)$$

where, η_{ele} = Electrical efficiency (dimensionless); I = Current (A); V = Voltage (V)

$$\eta_{PV/T} = \eta_{th} + \eta_{ele} \quad (3)$$

where, η_{PVT} = Overall efficiency (dimensionless).

The output power of the PV panel can be obtained using the following equation:

$$\dot{E}_{PV} = G \times \tau_g \times \alpha_{PV} \times A_{PV} \times \eta_r(1 - \beta_r(T_{PV} - T_r)) \quad (4)$$

where, $\dot{E}_{PV}$ = PV panel output power (W); τ_g = Glass transmittance coefficient (dimensionless); α_{PV} = PV cell absorptivity coefficient (dimensionless); η_r = Reference efficiency at standard test conditions (dimensionless); β_r = Temperature coefficient (K^{-1}); T_{PV} = PV cell temperature (K); T_r = Reference temperature (K); η_r denotes the reference electrical efficiency of the PV panel under Standard Test Conditions (STC), adjusted for temperature effects using the coefficient β_r.

To measure the current intensity and voltage passing through the system, a DC-DC step-down power module was utilized. A thermometer (TM-917, Lutron, Taiwan) was employed to read the temperatures recorded by the temperature sensors. Type K immersion sensors were used to measure the ambient and fluid temperatures, while Type K wired sensors were attached to the back of the panel to monitor its temperature. Data collection was conducted at 15-second intervals to ensure consistent measurements. Solar radiation per unit area was measured using a digital pyranometer (TES1333R, Taiwan) with a precision of 1 W m^{-2}.

In the preparation of the nanofluid, copper oxide nanoparticles with the specific structural properties detailed in Table 2 were used. The nanofluid was prepared at concentrations of 0.05% and 0.025%. The system featured a mechanism for transferring both nanofluid and water from a 20-liter cylindrical plastic tank specifically designed for storing these solutions. A 12 mm diameter hose was

employed to facilitate the flow of fluids through the system's inlets and outlets. A comparative analysis of the PVT system was conducted against the reference panel over a period of six consecutive days, with each day consisting of 6 hours of observation in October 2023. This evaluation included two different flow rates, 0.02 and 0.01 L s^{-1}, for the nanofluid at concentrations of 0.05% and 0.025%, as well as for pure water. The experimental procedures were carried out each day, focusing on one concentration level and one distinct flow rate within the Renewable Energy Laboratory at the University of Kurdistan. Each day, the system was initialized at 9:30 AM for experimentation and data collection, which occurred at 15-minute intervals until 3:30 PM.

Table 2- Properties of copper oxide nanoparticles used in the experiment (Amalraj & Michael, 2019)

Property	Description
Size of nanoparticles	20 nanometers
Purity percentage	99.9%
Appearance of nanoparticles	Spherical
Specific surface area	35 m^2 g^{-1}
Bulk density	0.79 g cm^{-3}
Particle density	6.4 g cm^{-3}

Measuring tools and uncertainty analysis considerations

In order to record data including temperature, solar radiation, relative humidity (for volume fraction), wind velocity, and the weight of the nanoparticles, a selection of instruments were used. The details of the instruments, considering the model, measuring range, least measuring unit, and uncertainty, are included in Table 3.

Table 3- Measuring tools used in the experiments and the details

Type of tools	Model	Measuring range	Least measuring unit	Uncertainty
Anemometer	AM-4206, Lutron	0.3–25 m s^{-1}	0.1 m s^{-1}	1%
Thermometer	TM-914C, Lutron	-100–100 °C	0.01 °C	1%
Hygrometer	HT.3006, Lutron	0–100%	0.1%	0.01%
Pyranometer	TES1333R, Lutron	1–2000 W m^{-2}	10 W m^{-2}	5%
Balancer	SJX1502N, Ohaus	1–1500 g	0.01 g	1%

During the period of experimentation, the validity of the measuring technique was validated through the application of uncertainty computations. Given that random error is unavoidable, unforeseeable, and manageable, it is chiefly responsible for the ambiguity in data measurement. Consequently, the measurements were conducted on a minimum of three occasions, with the mean data being factored in. The overall experimental uncertainty is quantifiable through the utilization of Eq. 5 (Ahmadi, Samimi Akhijahani, & Salami, 2024):

$$W_R = \sqrt{(\frac{\partial R}{\partial x_1} w_1)^2 + (\frac{\partial R}{\partial x_2} w_2)^2 + \ldots + (\frac{\partial R}{\partial x_n} w_n)^2} \quad (5)$$

where, w and R stand for the dimensional shape factor and the uncertainty function, respectively, and W_R displays the overall degree of uncertainty (%) of the findings. Additionally, w_n represents the unpredictability of the independent variables. The accuracy and measurement range of the data collection devices are given in Table 4.

Table 4- The factors applied to evaluate uncertainty of the test

Parameters	Solar radiation (W m^{-2})	Temperature (K)	Fluid mass flow rate (kg s^{-1})	Test method
Uncertainty (%)	2.1	0.1	0.5	3.21

Results and Discussions

The experimentation trials were conducted during typical summer days, i.e., 21 to 26 September 2023. As can be seen from Fig. 3, the data during trials were recorded in an unshaded area for the whole trial period. According to data recording procedure, the graphs have been plotted for depicting the trend of changes of solar radiation intensity and ambient temperature over the duration of 09:30 to 15:30. It was observed that the peak value of solar radiation was at a point of approximately 924±11 W m^{-2} at 11:45 local time. The minimum values were at both the beginning and termination of the experiment. However, ambient temperature followed a different trend compared to that of solar radiation and attained a peak value of around 31.15 °C at 14:00. The variations in airspeed observed on the test days were minimal, fluctuating between 0.2 and 0.9 m s^{-1}. Because of the low convective heat transfer coefficient, the impact on the process is considered negligible.

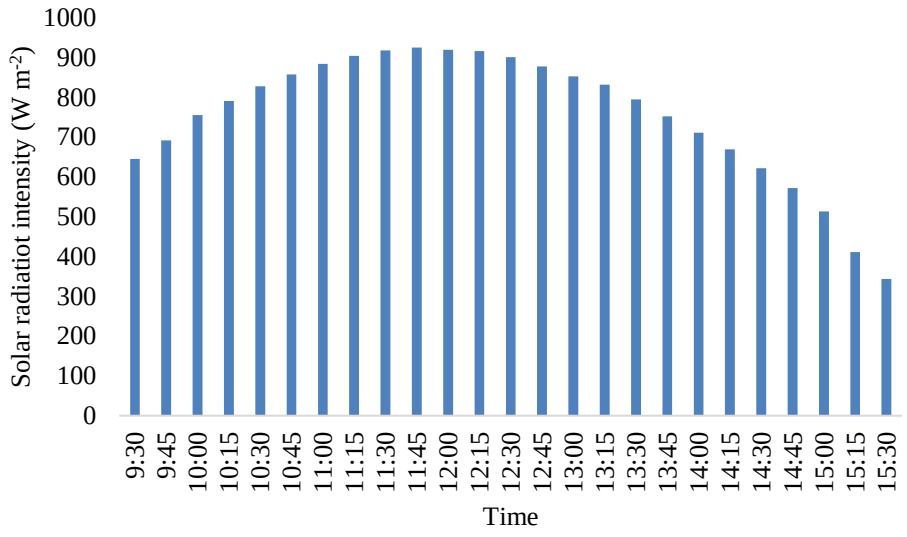

a

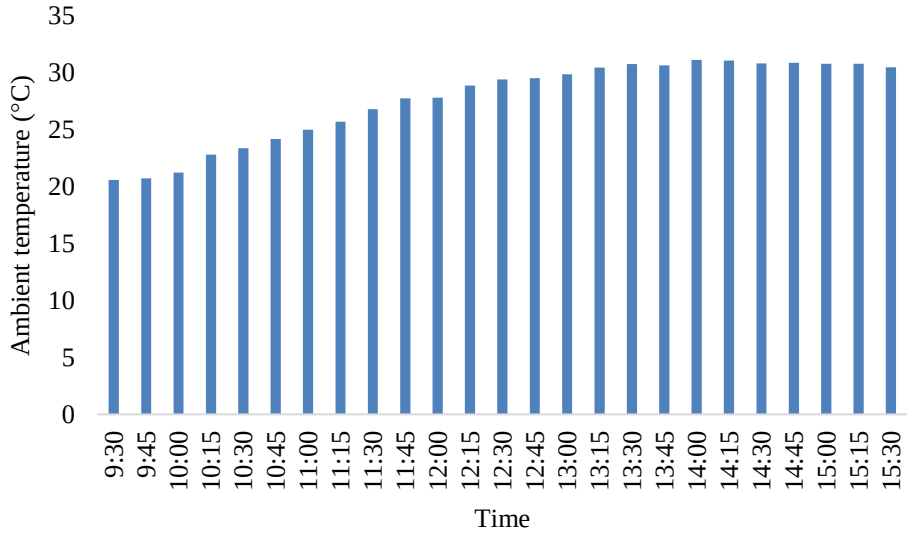

b

Fig. 3. The experimental data of (a) solar radiation intensity, and (b) ambient temperature

As illustrated in the graph shown in Fig. 4, both over time and with increasing irradiance intensity, the electrical efficiency of the reference panel exhibits a decline. This decrease can be attributed to the conversion of received light into heat and the resulting rise in the surface temperature of the panel. At peak radiation intensity of 924 W m^{-2}, the electrical efficiency of the reference panel was 12.8%. In contrast, under these conditions, the electrical efficiency of the PVT system was recorded at 9.99%. As the radiation intensity decreased later in the day, the ambient temperature also decreased, and the electrical efficiency of reference panels improved. By 3:30 PM, the reference panel achieved an electrical efficiency of 13.80%, while the PVT system reaches an efficiency of 8.81%. The PVT system also demonstrated its lowest and highest electrical efficiencies at 3:30 AM and 12:30 PM, respectively, with values of 8.81% and 10.21%.

The PVT system's lower electrical efficiency during initial and final periods (e.g., 14:15–15:30) arises from the interplay between cooling benefits and optical losses. At low irradiance, the shading effect of the nanofluid reduces light absorption, outweighing the cooling advantage. Conversely, at peak irradiance, cooling dominates, improving efficiency. The reference panel benefits from natural temperature reduction in the late afternoon, while the PVT system's active cooling becomes less impactful under diminishing solar input.

The reduced electrical efficiency of the PVT system during early and late experimental periods may also stem from optical losses, such as reflection and refraction at the glass-nanofluid interface, particularly under low solar angles. These losses compound the shading effect of the nanofluid, further reducing effective irradiance. Future studies could optimize chamber design (e.g., anti-reflective coatings, tilt adjustments) to minimize these losses.

The efficiency pattern of the reference panel demonstrates physically consistent behavior throughout the day. Starting at 9:30 with a peak efficiency of 14.10%, the panel's performance gradually decreases as the day progresses, reaching 12.80% at 11:45. This initial decline is primarily attributed to the increasing panel temperature as solar radiation intensifies and heat accumulates in the panel. The morning efficiency is highest because the panel starts cool from overnight conditions, allowing optimal photovoltaic conversion. As the day continues into midday (11:45-13:00),

the efficiency stabilizes at its lowest range (12.80-12.51%) due to maximum solar radiation and highest panel temperatures, which negatively impact voltage output and overall conversion efficiency. During the early afternoon period (13:00-15:30), as solar radiation decreases and ambient temperatures begin to moderate, the panel's efficiency gradually recovers from 12.51% to 13.80%. This afternoon recovery occurs because the panel begins to cool down, improving its voltage characteristics and conversion efficiency. This pattern aligns with the fundamental physics of photovoltaic panels, which exhibit a negative temperature coefficient, meaning their efficiency decreases as temperature rises.

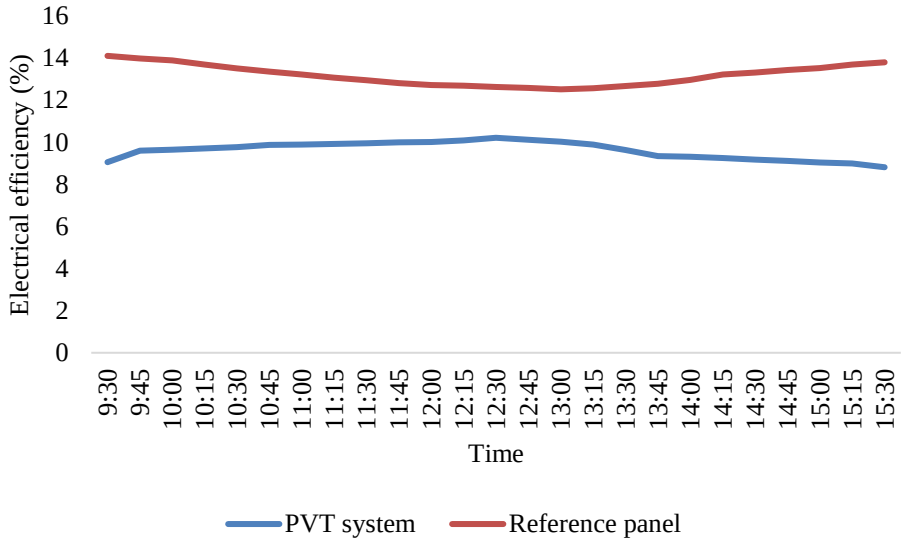

Fig. 4. Average electrical efficiency of the reference and the PVT systems over 6 days

According to Fig. 5, the temperature of the reference panel fluctuated over time in response to changes in irradiation intensity. Specifically, as solar radiation intensity increased, the temperature of the reference panel rose until it reached a maximum value, after which it began to decline. At 11:45 AM, when irradiation intensity peaked at 924 W m^{-2}, the reference panel's temperature reached its highest point of 50.75 °C, followed by a noticeable downward trend. In contrast, the PVT system exhibited an initial upward trend until 2:15 PM, when irradiation intensity was 669 W m^{-2}; it then reached its peak temperature of 39.97 °C before beginning to decrease. The lowest recorded temperatures for the reference and PVT systems in the early hours of the day were 34.30 °C and 22.70 °C, respectively. As anticipated, the presence of the cooling fluid (water or copper oxide nanofluid) resulted in a lower surface temperature for the PVT system, which was reflected in its temperature graph lying below that of the reference panel. The overall efficiency from the beginning to the end of the observation period showed minimum and maximum values of 15.97% and 46.49%, respectively. Notably, when the PVT system temperature peaked at 37.70 °C, the overall efficiency also reached its highest point. Meanwhile, when the temperature of the PVT system peaked at 39.97 °C at 2:15 PM, the overall efficiency for that panel was recorded at 30.16%. Following this peak, as temperatures declined, the efficiency notably increased. This trend also applied to thermal efficiency, which displayed an upward trajectory; when the system temperature was at its peak, the thermal efficiency measured 25.91%. As the temperature decreased, the thermal efficiency continued to rise, ultimately reaching a maximum value of 42.87% in the

late afternoon. In contrast, the pattern of electrical efficiency differed significantly. During the early morning hours, when the PVT system temperature was at its lowest at 22.70 °C, electrical efficiency peaked at 9.59%. However, as the system temperature rose and reached a high of 39.97 °C, electrical efficiency reached 10.18%. Then the downward trend continued until 3:30 PM, when efficiency hit its lowest point at 8.81%. The reason for the lesser increase in temperature for the PVT system, compared to the reference panel, can be attributed to the presence of the copper oxide nanofluid, which effectively mitigated temperature rise.

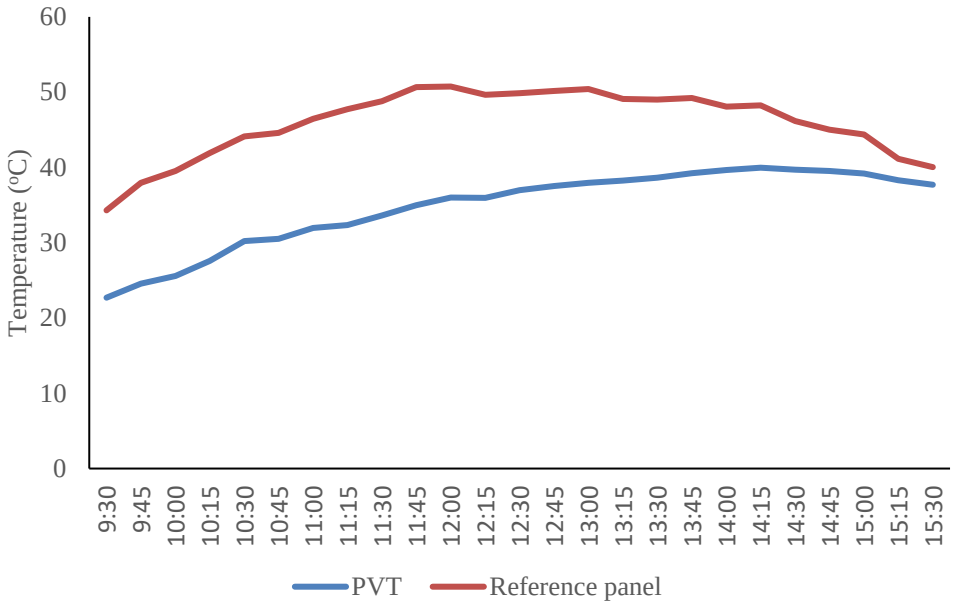

Fig. 5. Average temperature of the reference and the PVT systems over 6 days

Based on the data presented in Fig. 6, it is evident that as the surface temperature of the reference panel increased over time, the intensity of current gradually rose. This increase continued until 2:45 PM, when it peaked at 2.15 A. At this peak moment, the panel's surface temperature was notably high at 45.03 °C, while the voltage measured 20.35 V and the power nearly reached its maximum value of 43.75 W. Following this peak, the intensity of current exhibited a downward trend, reaching a minimum value of 1.69 A by 3:30 PM. In contrast, the voltage decreased until 1:45 PM, when it hit its lowest point of 20.22 V. After this point, the voltage began to increase slightly, but the overall trend remained downward.

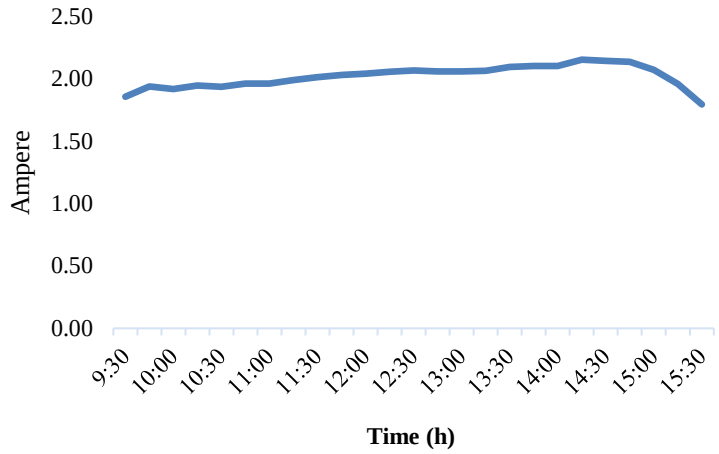

Fig. 6. Average current intensity of the reference panel over 6 days

Furthermore, the maximum values for both voltage and power were recorded at 9:30 AM, reaching 21.8 V and 43.67 W, respectively. At this point, the current intensity was 1.85 A, which was nearly at its peak level. Conversely, the minimum electrical efficiency of 6.56% was observed at 11:45 AM, during which the corresponding values for current, voltage, power, and temperature were 2.03 A, 20.27 V, 41.14 W, and 50.67 °C, respectively. Thus, it can be concluded that all three factors including current, voltage, and power, have a positive and direct impact on efficiency; as any of these increased or decreased, the electrical efficiency would similarly rise or fall. As shown in Table 5, the output efficiency when using water as a cooling fluid at flow rates of 0.01 and 0.02 L s^{-1} was measured at 22.56% and 26.35%, respectively. In contrast, when copper oxide nanofluid was employed as a coolant at a volume ratio of 0.05%, the output efficiency was 29.66% for a flow rate of 0.01 L s^{-1} and 40.72% for a flow rate of 0.02 L s^{-1}. When the volume ratio was reduced to 0.025%, the recorded output efficiency was 28.73% at a flow rate of 0.01 L s^{-1} and 39.67% at a flow rate of 0.02 L s^{-1}. This data indicated that copper oxide nanofluid had a more significant impact on output efficiency compared to water. Specifically, increasing the flow rate of copper oxide nanofluid enhanced the system's output efficiency. Also, for water, increasing the flow rate led to an increase in output efficiency. Moreover, the reduction of the volume ratio from 0.05% to 0.025% for the nanofluid correlated with an increase in output efficiency, which could be attributed to higher current and voltage intensities within the system.

When maintaining a constant volume ratio of 0.05% and varying flow rates, increasing the flow rate from 0.01 to 0.02 L s^{-1} yielded a thermal efficiency for the system using copper oxide nanofluid that surpassed that of the system utilizing water as a coolant. Specifically, the thermal efficiency values were 31.87% for the nanofluid and 18.53% for water, indicating that the heat transfer rate of copper oxide nanofluid was superior to that of water. However, the electrical efficiency of the system with copper oxide nanofluid (0.05%) was less than that of the system with copper oxide nanofluid (0.025%); at a flow rate of 0.02 L s^{-1}, the values were 8.85% for the 0.05% nanofluid and 10.02% for the 0.025% nanofluid. This discrepancy can be attributed to the lack of shading effects in nanofluid (0.025%), in contrast to the copper oxide nanofluid (0.05%), which has a dark color that reduces the visibility of the panel surface and therefore limits solar energy absorption. Despite this, the overall efficiency of the system employing copper oxide nanofluid was higher than that of the system with water, with overall efficiency values of 40.72% and 26.35%, respectively. Notably, for the water coolant, increasing the flow rate resulted in an improvement in the system's electrical

efficiency.

Table 5- Impact of flow rate on system efficiencies

Flow Rate (L s^{-1})	Electrical Efficiency (with copper oxide 0.025%)	Thermal Efficiency (with copper oxide 0.025%)	Overall Efficiency (with copper oxide 0.025%)	Electrical Efficiency (with copper oxide 0.05%)	Thermal Efficiency (with copper oxide 0.05%)	Overall Efficiency (with copper oxide 0.05%)	Electrical Efficiency (with water)	Thermal Efficiency (with water)	Overall Efficiency (with water)
0.01	9.26%	19.47%	28.73%	8.55%	21.11%	29.66%	7.79%	14.77%	22.56%
0.02	10.02%	29.65%	39.67%	8.85%	31.87%	40.72%	7.82%	18.53%	26.35%

At a constant flow rate of 0.01 L s^{-1}, increasing the copper-oxide nanofluid volume ratio to 0.05% enhanced electrical, thermal, and overall efficiencies relative to water. As the volume ratio of the nanofluid decreased from 0.05% to 0.025%, the thermal efficiency of the system declined from 21.11% to 19.47%, while the overall efficiency decreased from 29.66% to 28.73%. Higher volume ratios of nanofluid did not enhance electrical efficiency; in fact, they resulted in a decline in electrical efficiency when the volume ratio exceeded 0.025%. However, reducing the volume ratio of copper oxide nanofluid could improve electrical efficiency, although it still has superiority to the efficiency of pure water. As the volume ratio neared that of water, the efficiency of the nanofluid system increased correspondingly. Conversely, as the volume ratio decreased, the color of the copper oxide nanofluid became less dark and more transparent, which enhanced its efficiency. Thus, optimizing the volume ratio of the nanofluid was crucial for improving the system's overall performance. At a constant flow rate of 0.02 L s^{-1}, the results were similar. Specifically, reducing the copper oxide concentration from 0.05% to 0.025% led to an increase in electrical efficiency. But thermal efficiency decreased from 31.87% to 29.65%, while electrical efficiency improved from 8.85% to 10.02%. As a result, the overall efficiency of the system demonstrated a similar trend of thermal efficiency, decreasing from 40.72% to 39.67%. Thus, the decrease in the volume ratio of copper oxide nanofluid reduced the overall and thermal efficiencies. When the copper oxide volume ratio was at 0.025%, the thermal and overall efficiencies of the system exceeded those of the water-based system. Also, the electrical efficiency remained higher, indicating that the presence of copper oxide nanofluid enhanced electrical output compared to water, ultimately resulting in higher power production.

At both flow rates of 0.01 and 0.02 L s^{-1}, the electrical efficiency of the system utilizing copper oxide nanofluid as a coolant consistently outperformed that of the system using water. Also, for thermal and overall efficiencies at a flow rate of 0.02 L s^{-1}, the systems with copper oxide coolant demonstrated superior performance compared to those using water, regardless of whether the volume ratio was 0.05% or 0.025%. Similarly, at a lower flow rate of 0.01 L s^{-1}, the thermal and overall efficiencies of the copper oxide-cooled system exceeded those of the water-cooled system. Thus, the copper oxide nanofluid coolant exhibited better electrical, thermal, and overall performance at flow rates of 0.01 and 0.02 L s^{-1}.

According to Table 6, as the flow rate increased, the average temperature difference between the reference panel and the PVT system consistently rose, regardless of the volumetric ratio of the coolant. This trend could be attributed to the increased flow rate of the specific fluid, which allowed for greater heat absorption and subsequently lowered the temperature of the system. As a result, the temperature difference between the reference panel and the PVT system widened. Additionally, the average thermal efficiency showed a clear upward trend in its decrease over the course of the experiment, with values

noticeably increasing. Specifically, while thermal efficiency declined on all days of the experiment except for the first day, the overall pattern indicated a significant reduction in average thermal efficiency as the experiment progressed.

Table 6- Average temperature difference between the reference panel and the PVT system at varying flow rates

	Flow rates	
Type of fluid	**0.01 L s^{-1}**	**0.02 L s^{-1}**
Copper oxide nanofluid 0.025%	10.77 ℃	11.29 ℃
Copper oxide nanofluid 0.05%	11.18 ℃	11.80 ℃
Water	8.35 ℃	9.42 ℃

Additionally, the higher thermal efficiency reflects the nanofluid's superior capability to dissipate heat, which benefits thermal energy capture but does not directly enhance electrical output at higher concentration ratios. This trade-off highlights the need to optimize nanofluid composition and optical properties to balance thermal and electrical performance in PVT systems.

Conclusion

This study investigated the impact of copper oxide nanofluid and water on the thermal and electrical efficiency of a photovoltaic thermal system, revealing several key insights. Overall, the electrical efficiency of the control panel was found to be lower than that of the systems utilizing both coolant types (water and copper oxide nanofluid). Also, the systems using copper oxide nanofluid at both concentrations of 0.025% and 0.05% exhibited higher electrical efficiency compared to water-cooling systems. However, the electrical efficiency of copper oxide nanofluid at a concentration of 0.025% was higher than 0.05%. This observation highlights the influence of the darker color of the copper oxide nanofluid on light absorption. A reduction in the volume percentage of copper oxide from 0.05% to 0.025% resulted in improved electrical efficiencies, attributed to the clearer fluid allowing for greater light penetration to the panel surface. Furthermore, increasing the flow rate from 0.01 to 0.02 L s^{-1} significantly enhanced the thermal and overall performance of the copper oxide nanofluid system, as this change facilitated increased heat absorption from the panel surface and contributed to lower panel temperatures. More study has to be done to examine the optimization of nanofluids' concentrations for even better electrical efficiency, e.g., testing with different nanoparticles with greater transparency or various concentrations of fluids for lowering shading effects such as Al_2O_3. Long-term stability and environmental effect assessments define the commercial viability of nanofluid-based cooling systems. Furthermore, guaranteeing the availability of relevant information for significant acceptance into renewable energy systems calls for scaling of this technology up to large-scale systems and application in hybrid energy solutions.

Authors Contribution

M. Ghaderi: Data acquisition, Data pre and post processing, Software services

P. Salami: Supervision, Conceptualization, Methodology, Technical advice, Text mining, Writing the original text

H. Samimi-Akhijahani: Conceptualization, Methodology, Statistical analysis, Software services, Numerical/computer simulation

S. Zareei: Conceptualization, Methodology, Validation

M. Safvati: Visualization, Review and editing services

References

1. Ahmadi, M., Samimi Akhijahani, H., & Salami, P. (2024). Evaluation the performance of

drying efficiency and energy efficiency of a solar dryer quipped with phase change materials and air recirculation system. *Iranian Food Science and Technology Research Journal, 20(2)*, 199-216. https://doi.org/10.22067/ifstrj.2023.79695.1218

2. Ahmed, A., Baig, H., Sundaram, S., & Mallick, T. K. (2019). Use of nanofluids in solar PVThermal systems. *International Journal of Photoenergy*, 2019. https://doi.org/10.1155/2019/8039129
3. Al-Ezzi, A. S., & Ansari, M. N. M. (2022). Photovoltaic solar cells: A review. *Applied System Innovation*, *5*(4), 67. https://doi.org/10.3390/asi5040067
4. Al-Ghezi, M. K., Abass, K. I., Salam, A. Q., Jawad, R. S., & Kazem, H. A. (2021, August). The possibilities of using nano-CuO as coolants for PVT system: An experimental study. *Journal of Physics: Conference Series*, *1973*(1), 012123. IOP Publishing.
5. Alktranee, M., Shehab, M. A., Németh, Z., Bencs, P., & Hernadi, K. (2023). Experimental study for improving photovoltaic thermal system performance using hybrid titanium oxide-copper oxide nanofluid. *Arabian Journal of Chemistry*, *16*(9), 105102. https://doi.org/10.1016/j.arabjc.2023.105102
6. Allaker, R. P., & Yuan, Z. (2019). *Chapter 10 - Nanoparticles and the control of oral biofilms*. PP 243-275 in K. Subramani and W. Ahmed eds. Micro and Nano Technologies, Nanobiomaterials in Clinical Dentistry (Second Edition), Elsevier. https://doi.org/10.1016/B978-0-12-815886-9.00010-3
7. Amalraj, S., & Michael, P. A. (2019). Synthesis and characterization of Al_2O_3 and CuO nanoparticles into nanofluids for solar panel applications. *Results in Physics*, *15*, 102797. https://doi.org/10.1016/j.rinp.2019.102797
8. Arefin, M. A. (2019). Analysis of an integrated photovoltaic thermal system by top surface natural circulation of water. *Frontiers in Energy Research*, *7*, 97. https://doi.org/10.3389/fenrg.2019.00097
9. Brahim, T., & Jemni, A. (2017). Economical assessment and applications of photovoltaic/thermal hybrid solar technology: A review. *Solar Energy*, *153*, 540-561. https://doi.org/10.1016/j.solener.2017.05.081
10. Dubey, S., Sarvaiya, J. N., & Seshadri, B. (2013). Temperature dependent photovoltaic (PV) efficiency and its effect on PV production in the world–a review. *Energy Procedia*, *33*, 311-321. https://doi.org/10.1016/j.egypro.2013.05.072
11. Elias, B. H., AlSadoon, S. H. M., & Abdulgafar, S. A. (2014). Modeling and Simulation of Photovoltaic Module Considering an Ideal Solar Cell. *International Journal of Advanced Research in Physical Science*, *1*(3), 9-18.
12. Haidar, Z. A., Orfi, J., & Kaneesamkandi, Z. (2018). Experimental investigation of evaporative cooling for enhancing photovoltaic panels' efficiency. *Results in Physics*, *11*, 690-697. https://doi.org/10.1016/j.rinp.2018.10.016
13. Idoko, L., Anaya-Lara, O., & McDonald, A. (2018). Enhancing PV modules efficiency and power output using multi-concept cooling technique. *Energy Reports*, *4*, 357-369. https://doi.org/10.1016/j.egyr.2018.05.004
14. Joshi, S. S., Andhare, A. M., Bhave, N. A., & Gudadhe, N. P. (2019). Thermal management of photovoltaic systems: Case studies. *Journal of Physics: Conference Series*, *1240*(1), 012021. IOP Publishing.
15. Khalili, Z., & Sheikholeslami, M. (2024). Simulation of CuO-water nanofluid flow for cooling of solar photovoltaic module. *Numerical Heat Transfer, Part A: Applications*, 1-12. https://doi.org/10.1080/10407782.2024.2350028
16. Madas, S. R., Narayanan, R., & Gudimetla, P. (2023). Numerical investigation on the optimum performance output of photovoltaic thermal (PVT) systems using nano-copper oxide (CuO) coolant. *Solar Energy*, *255*, 222-235. https://doi.org/10.1016/j.solener.2023.02.035

17. Mirzaee, P., Salami, P., Samimi Akhijahani, H., & Zareei, S. (2023). Life cycle assessment, energy and exergy analysis in an indirect cabinet solar dryer equipped with phase change materials. *Journal of Energy Storage, 61*, 106760. https://doi.org/10.1016/j.est.2023.106760
18. Mohammadi Sarduei, M., Mortezapour, H., & Jafari Naeimi, K. (2017). Numerical analysis of using hybrid photovoltaic-thermal solar water heater in Iran. *Journal of Agricultural Machinery, 7*(1), 221-233. https://doi.org/10.22067/jam.v7i1.47426
19. Pordanjani, A. H., Aghakhani, S., Afrand, M., Sharifpur, M., Meyer, J. P., Xu, H., …, & Cheraghian, G. (2021). Nanofluids: Physical phenomena, applications in thermal systems and the environmental effects—a critical review. *Journal of Cleaner Production, 320*, 128573. https://doi.org/10.1016/j.jclepro.2021.128573
20. Salami, P., Ajabshirchi, Y., Abdollahpoor, S., & Behfar, H. (2016). A comparison among different parameters for designing a photovoltaic/thermal system using computational fluid dynamics. *Engineering, Technology & Applied Science Research, 6*(5), 1119-1123. https://doi.org/10.48084/etasr.667
21. Sardarabadi, Passandideh-Fard, M., & Zeinali Heris, M. (2014). Experimental investigation of the effects of silica/water nanofluid on PVT (photovoltaic thermal units). *Energy, 66*, 264-272. https://doi.org/10.1016/j.energy.2014.01.102
22. Sathe, T. M., & Dhoble, A. S. (2017). A review on recent advancements in photovoltaic thermal techniques. *Renewable and Sustainable Energy Reviews, 76*, 645-672. https://doi.org/10.1016/j.rser.2017.03.075
23. Sheeba, K. N., Rao, R. M. & Jaisankar, S. (2015). A study on the underwater performance of a solar photovoltaic panel. *Energy Sources, Part A: Recovery, Utilization, and Environmental Effects, 37*(14), 1505-1512. https://doi.org/10.1080/15567036.2011.619632
24. Siah Chehreh Ghadikolaei, S. (2021). Solar photovoltaic cells performance improvement by cooling technology: An overall review. *International Journal of Hydrogen Energy, 46*(18), 10939-10972. https://doi.org/10.1016/j.ijhydene.2020.12.164
25. Tina, G. M., Rosa-Clot, M., Rosa-Clot, P., & Scandura, P. F. (2012). Optical and thermal behavior of submerged photovoltaic solar panel: SP2. *Energy, 39*(1), 17-26. https://doi.org/10.1016/j.energy.2011.08.053
26. Yazdanifard, F., Ameri, M., & Ebrahimnia-Bajestan, E. (2017). Performance of nanofluid-based photovoltaic/thermal systems: A review. *Renewable and Sustainable Energy Reviews, 76*, 323-352. https://doi.org/10.1016/j.rser.2017.03.025

بررسی تاثیر ترکیب نانوذرات اکسید مس و آب مقطر بر راندمان یک سامانه فتوولتاییک حرارتی

مهری قادری[۱]، پیمان سلامی[۱*]، هادی صمیمی اخیجهانی[۱]، سمیرا زارعی[۱]، محمد صفوتی[۲]

تاریخ دریافت: ۱۴۰۳/۱۲/۱۴
تاریخ پذیرش: ۱۴۰۴/۰۳/۱۲

چکیده

رشد سریع جمعیت جهان و افزایش تقاضا برای انرژی، همراه با نیاز فوری به حفاظت از محیط‌زیست، محققان را بر آن داشته است تا منابع انرژی تجدیدپذیر را به‌عنوان جایگزینی مناسب برای سوخت‌های فسیلی تجدیدناپذیر بررسی کنند. این مطالعه بهبود عملکرد سیستم‌های فتوولتاییک حرارتی (PVT)را با استفاده از روش خنک‌کننده غوطه‌وری با نانوسیال‌های اکسید مس ارزیابی می‌کند. دستگاه آزمایشی شامل یک محفظه شیشه‌ای بود که سطح پنل خورشیدی در زیر آن غوطه‌ور شده بود. آزمایش‌ها در نسبت حجمی نانوسیال ۰/۰۲۵۰٪ و ۰/۰۵٪ و نرخ جریان ۰/۰۱ و ۰/۰۲ لیتر در ثانیه انجام شد. ارتفاع غوطه‌ور شدن در داخل محفظه شیشه‌ای ۵ سانتی‌متر بود. آزمایش‌ها در شرایط محیطی که شامل دمای محیط ۲۰/۶–۳۱/۲ درجه سلسیوس و تابش ۳۴۳–۹۲۴ وات بر مترمربع انجام شد. نتایج نشان داد که نانوسیال‌های اکسید مس در نسبت حجمی ۰/۰۵ درصد و سرعت جریان ۰/۰۲ لیتر بر ثانیه، راندمان حرارتی را به ۳۱/۸۷ درصد بهبود داده و دمای سطح پانل را تا ۱۱/۸ درجه سلسیوس در مقایسه با خنک‌کننده آب کاهش داده است. همچنین راندمان الکتریکی سامانه PVT از پنل مرجع فراتر رفت. راندمان کلی سیستم PVT به ۴۱/۸۹ درصد رسید. این یافته‌ها پتانسیل خنک‌سازی مبتنی بر نانوسیال را برای بهینه‌سازی راندمان سامانه PVT با افزایش مدیریت حرارتی نشان می‌دهد.

واژه‌های کلیدی: خنک‌کنندگی، دمای سامانه، راندمان حرارتی، غوطه‌وری، نانوسیال اکسید مس

۱– گروه مهندسی بیوسیستم، دانشکده کشاورزی، دانشگاه کردستان، سنندج، ایران
۲– گروه مهندسی بیوسیستم، دانشکده کشاورزی، دانشگاه صنعتی اصفهان، اصفهان، ایران
(*– نویسنده مسئول: Email: p.salami@uok.ac.ir)

https://doi.org/10.22067/jam.2025.92457.1349